Artificial Zinc Enzymes with Fine-Tuned Catalytic Active Sites for Highly Selective Hydrolysis of Activated Esters

MD Arifuzzaman and Yan Zhao*

Department of Chemistry, Iowa State University, Ames, Iowa 50011-3111

ABSTRACT: Zinc enzymes are ubiquitous in nature and frequently used to catalyze the hydrolysis of carboxylic acid esters, phosphate esters, and amides. Although many models and mimics of zinc enzymes have been reported, it remains difficult to construct active sites with accurately positioned catalytic groups and tunable substrate selectivity. By imprinting a substrate-like amino template coordinated to a polymerizable zinc complex inside cross-linked micelles, we prepared water-soluble nanoparticles with well-defined active sites. The position of the zinc ion could be tuned systematically with respect to the ester bond to be leaved in the substrate (*p*-nitrophenyl esters), as well as the rigidity of the active site. Our imprinted zinc catalysts was able to distinguish substrates that differed by the position of a single methyl group, chain length of the acyl chain, and substitution of the phenyl ring. The turnover number (>460 at pH 7) was one order of magnitude higher than those previously reported for artificial zinc enzymes in the literature.

KEYWORDS: *molecular imprinting, hydrolysis, artificial enzyme, selectivity, Michaelis-Menten, active site, biomimetic catalysis*

INTRODUCTION

Zinc is used by >1000 enzymes to perform vital catalytic tasks in biology.[1,2] Of these enzymes, the largest group is hydrolases that catalyze the hydrolysis of carboxylic acid esters, peptides, and phosphate esters under physiological conditions.[3,4] In the last decades, numerous small-molecule zinc complexes have been synthesized to mimic the coordination environments of zinc in the natural enzymes and understand its potential role in the catalysis.[5-7] Reproducing their catalytic behavior in aqueous solution, however, is hampered by the poor water solubility of common organic ligands, dimerization of zinc complexes, and product inhibition.[8]

To overcome these challenges, researchers turned to peptidic materials in recent years to construct artificial zinc enzymes and have synthesized by far the most active mimics of the natural catalysts.[8-13] Peptidic structures have a number of attractive features for biomimetic catalysis. Aqueous solubility, for example, can be easily achieved. Identical ligands such as histidine and aspartate found in the zinc enzymes could be used to bind the metal to better simulate the coordination environments. Steric protection by the peptide framework can prevent the dimerization of zinc complexes effectively. Indeed, with a zinc ion placed in the hydrophobic region of protein interfaces,[9,11] coiled coils,[8,10] self-assembled amyloid fibers,[12] or α-helical barrels,[13] Michalis-Menten kinetics has been observed in the hydrolysis of model substrates. For the most commonly used activated ester *para*-nitrophenyl acetate (PNPA), the catalytic efficiency often came close to that of carbonic anhydrase, a natural zinc enzyme.

One of the biggest challenges forward in the creation of artificial enzymes is in the design of the active site. For bottom-up-constructed small-molecule enzyme models, tremendous synthetic efforts are needed for a highly functionalized binding pocket, especially if water-solubility, steric protection, and other features all need to be included. Although a large database of naturally folded structures, automated synthesis, and computational tools are available to peptide-based materials, fine-tuning of the active site for substrates of different shapes remains a formidable task.

Herein, we report a rational, facile construction of artificial zinc enzymes by a bottom-up approach through micellar imprinting.[14] Although molecularly imprinted catalysts are known in the literature,[15-24] traditional molecularly imprinted polymers (MIPs) face a number of challenges[25] to be used as mimics of natural enzymes, partly due to limited precision in the construction of the active sites, heterogeneous distribution of the binding sites, and/or poor solubility of highly cross-linked materials. Our molecularly imprinted nanoparticle (MINP) catalysts are characterized by their resemblance to natural enzymes in the nanodimension and water-solubility. The discrete active site, tunable in size and shape, is located in the hydrophobic core of the MINP. The highlight of our method is the systematic tuning of the catalytic zinc metal with respect to the ester bond to be cleaved in the substrate. The shape of the active site could be made to match the substrate precisely, to the point that the position of a single methyl group and the chain length of the substrate could be distinguished with ease. Artificial zinc enzymes often face strong product inhibition because the hydrolyzed products coordinate to zinc more strongly than the starting materials.[8] In our catalysts, product inhibition was effectively prevented, resulting in turnover numbers one order of magnitude higher than those reported in previous systems.

RESULTS AND DISCUSSION

Design and Synthesis of Zn Catalysts. Scheme 1 illustrates the preparation of our artificial zinc enzymes. Cross-linkable surfactant **1** has two sets of orthogonal reactive groups—the tripropargyl groups in the head for surface-cross-linking with diazide **2** by the click reaction and the methacrylate on the hydrophobic tail for

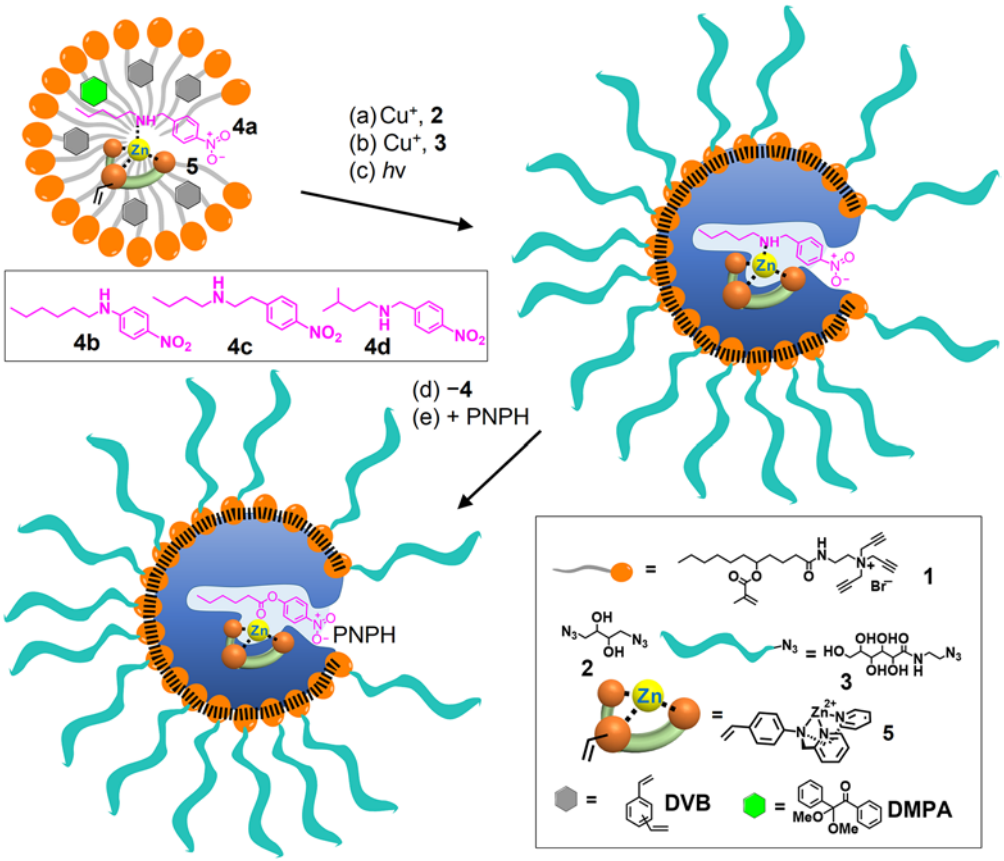

Scheme 1. Preparation of catalytic Zn-MINP as an artificial esterase for PNPH hydrolysis.

core-cross-linking with divinyl benzene (DVB) by free radical polymerization.[14] Surface ligand **3** is generally added after the surface-cross-linking, to decorate the cross-linked micelles with a layer of hydrophilic groups.[26] The entire synthesis was a one-pot reaction complete in less than two days and the procedures have been described in our previous publications.[14,27-29] Generally, the surface and core-cross-linking were monitored by ^{1}H NMR spectroscopy. The size and molecular weight of the MINP were measured by dynamic light scattering (DLS). The DLS size has been confirmed by transmission electron microscopy (TEM, Figure S13). The surface cross-linking has been verified by mass spectrometry after cleavage of the 1,2-diol surface cross-linkages by periodate.[26] Formation of the templated binding pockets has been confirmed by fluorescence titration and/or isothermal titration calorimetry (ITC) for many different types of templates.[14,30-33]

Amines **4a**–**4d** are the templates used in this study. Their complexation with functional monomer (FM) **5** fixes the position of the amino nitrogen with respect to Zn^{2+}. The tridentate ligand has been a popular zinc-binding motif.[3] The surface/core double-cross-linking of the micelle then fixes the position of the zinc ion in the pocket, which is shaped as the template by the molecular imprinting process. Templates **4a**–**4c** are all designed to mimic the hydrolytic substrate *para*-nitrophenyl hexanoate (PNPH) in size and shape. We used the amines as the template to mimic PNPH because they are better ligands for the zinc complex than the activated ester itself and hydrolytically stable in the presence of zinc.

In the literature, PNPA is the most commonly used substrate in artificial zinc enzymes.[8-13] We chose to use PNPH to test our design of the active site and its selectivity, because we wanted to modify the alkyl chain and examine its effect on the catalysis (vide infra). The difference of **4a**–**4c** is in the position of the nitrogen on the alkyl chain. Through these templates, we can adjust the position of zinc systematically with respect to the ester group of PNPH to be bound in the active site. Additionally, we can tune the shape of the active site, independent of the zinc position using branched template **4d** as an example.

Binding Properties of Zn Catalysts. Although the micellar imprinting has worked successfully for many templates including hydrophobic sulfonates and carboxylates,[14,34] carbohydrates,[30,32] and peptides,[29,31,35] this is the first time a metal complex was installed in the cross-linked micelle. We were not sure whether the metal complexes would survive the double cross-linking to afford the amine-imprinted binding pocket.

To gain insight into the metal-assisted molecular imprinting,[36-38] we first studied the binding of the Zn-containing MINP by ITC, one of the most reliable methods to measure intermolecular interactions in solution.[39] When we studied the binding of fluorescent guest molecules by MINPs in many previous examples, the ITC-determined binding constants generally showed excellent agreements with those determined by fluorescence titrations.[14,31,33,40]

As shown in Table 1, Zn-MINP prepared with **4a** as the template bound its template in 25 mM HEPES buffer (pH 7.0) with a binding constant (K_a) of (24.0 ± 1.1) × 10^4 M^{-1}. The buffer was the same as

Table 1. Binding data for Zn-MINP in 25 mM HEPES buffer (pH 7.0) obtained by ITC.[a]

Entry	Host	Guest	K_a ($\times 10^4$ M^{-1})	N	-ΔG (kcal/mol)	-ΔH (kcal/mol)	TΔS (kcal/mol)
1	Zn-MINP(**4a**)	**4a**	23.9 ± 0.9	0.9 ± 0.2	7.3	1.4 ± 0.3	5.9
2	Zn-MINP(**4a**)	**4b**	4.3 ± 0.2	0.9 ± 0.1	6.3	1.1 ± 0.1	5.2
3	Zn-MINP(**4a**)	**4c**	8.9 ± 0.1	0.9 ± 0.2	6.7	1.5 ± 0.1	5.2
4	Zn-MINP(**4a**)	**4d**	6.8 ± 0.2	0.9 ± 0.2	6.6	2.4 ± 0.4	4.2
5	Zn-MINP(**4b**)	**4b**	10.0 ± 0.2	1.0± 0.2	6.8	4.9 ± 0.2	1.9
6	Zn-MINP(**4c**)	**4c**	17.0 ± 1.1	1.0 ± 0.1	7.1	9.1 ± 0.1	-2.0
7	Zn-MINP(**4d**)	**4d**	26.2 ± 0.9	0.9 ± 0.2	7.4	1.8 ± 0.3	5.3
8	Zn-MINP(**4d**)	**4a**	6.9 ± 0.1	1.1 ± 0.1	6.6	0.8 ± 0.01	5.8

[a] The titrations were generally performed in duplicates and the errors between the runs were <10%. N was the number of binding site per nanoparticle. All MINPs were prepared with a 1:1 ratio between the cross-linkable surfactant and DVB.

that used in the hydrolysis (vide infra). The binding site also had a reasonable level of selectivity, with K_a 3–6-fold lower for the other amine guests (**4b**–**4d**) than for template **4a** (Table 1, entries 1–4). These results confirmed that molecular imprinting occurred successfully and the binding site of the MINP was able to distinguish the shift of the amino nitrogen or the shift of the methyl group by 1 carbon.

Zn-MINP(**4a**) bound **4b** more weakly than **4c**, even though both amines has a mismatch of the nitrogen by 1 carbon from the original template. The most likely reason for this probably was the weaker electron-donating power of amine **4b** from its *para*-nitro group. This conclusion was verified by determining the binding of **4b** by its own imprinted receptor, i.e., Zn-MINP(**4b**): the binding constant (9.9×10^4 M^{-1}) was 1.7–2.4 times weaker than that of **4a** by Zn-MINP(**4a**) or **4c** by Zn-MINP(**4c**).

It should be mentioned that our ITC titrations consistently showed an average of 0.9–1.1 binding sites (N) per nanoparticle. We were able to control this number by keeping the ratio between the surfactant and the template the same as the micelle aggregation number (~50). If needed, the number of binding sites could be tuned using different surfactant/template ratio.[14]

To further confirm the binding selectivity, we prepared Zn-MINP(**4d**), from the branched amine template. It bound its template (**4d**) better than the mismatched **4a** by a ratio of 26:6.9 or 3.8:1 (entries 7–8). Thus, the imprinting was very reliable and the imprinted micelle always preferred the original template, branched or linear. The results also suggest both the position of the nitrogen and the shape of the substrate were important to the binding of the zinc-functionalized MINPs.

The binding data reported in Table 1 were all obtained in 25 mM HEPES buffer at pH 7. We have also determined the binding in water and the difference between the two sets of binding data were within 10–20% and all the trends discussed above remained the same (Table S1). We have repeatedly found that normally pH-sensitive bindings become less sensitive (on insensitive) inside MINP. Examples include the binding of peptides containing multiple acid and basic groups[31,35] and carbohydrates by boronic acids.[30,32]

Activity and Selectivity of Zn Catalysts. *p*-Nitrophenyl esters are frequently used as the substrates for zinc enzyme mimics, even though they are not natural substrates for zinc enzymes.[8-13] The reason for the choice was their high activity and convenient monitoring of hydrolysis by the UV absorption of the phenoxide product at 400 nm. As shown in Figure 1, PNPH hydrolyzed very slowly in 25 mM HEPES buffer (pH 7.0) at 40 °C, in the presence of FM **5** or nonimprinted nanoparticles prepared without the template and FM. (The hydrolysis with or without FM **5** in buffer was essentially the same.) In the presence of the same concentration of Zn-MINP(**4a**), however, the hydrolysis occurred rapidly, indicating that both MINP and the zinc ion were needed for the catalysis.[41,42]

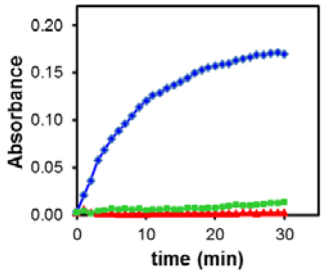

Figure 1. Absorbance at 400 nm as a function of time for the hydrolysis of PNPH in a 25 mM HEPEs buffer (pH 7.0) at 40 °C. The data sets correspond to hydrolysis catalyzed by Zn-MINP(**4a**) (◆), zinc complex **5** (▲), and nanoparticles prepared without **4a** and **5** (■). The data for the background hydrolysis in the buffer overlapped with those with **5** (▲) and were not shown for clarity of the figure. [PNPH] = 40 μM. [catalyst] = 8 μM.

Table 2 shows that, with 1 equiv DVB, Zn-MINP(**4a**) catalyzed the hydrolysis of PNPH with a pseudo-first-order rate constant of $k = 1.21 \times 10^{-4}$ s^{-1} in 25 mM HEPES buffer (pH 7.0) at 40 °C. Interestingly, as shown by entries 4 and 5, the reaction slowed down when the amino nitrogen of the template moved either to the right (in **4b**) or left (in **4c**). The result shows that the activity of our artificial zinc enzyme could be tuned by the position of the amino nitrogen in the template, as we had hypothesized. In addition, the catalytic activity could be tuned by the shape of the active site. Zn-MINP(**4d**), prepared from the branched template, showed a slower reaction in the hydrolysis of PNPH (entry 6).

When we constructed MINPs as receptors, we typically kept the ratio of DVB to the cross-linkable surfactant at 1:1 because an earlier study showed that the high level of DVB gave the micellar core rigidity essential to the binding selectivity.[14] This amount of DVB was the

highest the surfactant can solubilize in water. In this study, we reasoned that some flexibility might be important to the fast binding of the substrate and the release of the product and thus varied the amount of DVB used in the MINP preparation.

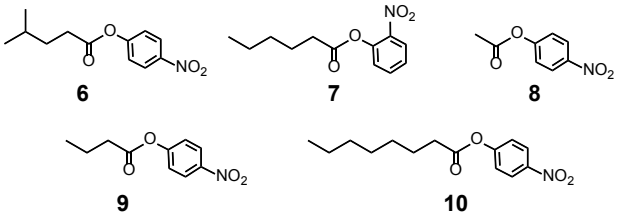

Table 2. Pseudo-first-order rate constants for the hydrolysis of activated esters catalyzed by Zn-MINPs in 25 mM HEPES buffer (pH 7.0).[a]

Entry	Catalyst	DVB:**1**	Substrate	k ($\times 10^{-4}$ s^{-1})
1	Zn-MINP(**4a**)	1:1	PNPH	1.21 ± 0.11
2	Zn-MINP(**4a**)	0.5:1	PNPH	4.31 ± 0.19
3	Zn-MINP(**4a**)	0:1	PNPH	0.71 ± 0.06
4	Zn-MINP(**4b**)	1:1	PNPH	0.68 ± 0.09
5	Zn-MINP(**4c**)	1:1	PNPH	0.89 ± 0.08
6	Zn-MINP(**4d**)	1:1	PNPH	1.01 ± 0.08
7	Zn-MINP(**4d**)	0.5:1	PNPH	0.89 ± 0.08
8	Zn-MINP(**4d**)	0:1	PNPH	1.10 ± 0.08
9	Zn-MINP(**4a**)	0.5:1	**6**	--[b]
10	Zn-MINP(**4a**)	0.5:1	**7**	--[b]
11	Zn-MINP(**4a**)	0.5:1	**8**	0.70 ± 0.04
12	Zn-MINP(**4a**)	0.5:1	**9**	0.48 ± 0.05
13	Zn-MINP(**4a**)	0.5:1	**10**	0.58 ± 0.04
14	none	-	**8**	0.21 ± 0.01
15	none	-	**9**	0.14 ± 0.01
16	none	-	PNPH	0.07 ± 0.01
17	none	-	**10**	0.06 ± 0.005
18	Zn-MINP(**4d**)	1:1	**6**	2.46 ± 0.14
19	Zn-MINP(**4d**)	0.5:1	**6**	7.15 ± 0.15
20	Zn-MINP(**4d**)	0:1	**6**	0.51 ± 0.04

[a] Reaction rates were measured in 25 mM HEPES buffer at 40 °C and pH 7.0. [PNPH] = 40 μM. [catalyst] = 8.0 μM unless otherwise indicated. The numbers given were averages from triplicate titrations at the 90% confidence level. [b] The hydrolysis was negligible under the reaction conditions.

The hypothesis was confirmed. Zn-MINP(**4a**) was optimized for PNPH, with its template resembling the substrate closely in size and shape. Cutting the amount of DVB by half increased the rate by 3.6-fold. Eliminating DVB decreased the rate by 1.7-fold (Table 1, entries 1–3).

Interestingly, when the active site was not optimized—i.e., when Zn-MINP(**4d**) was used to catalyze the hydrolysis of PNPH—the activity of the catalyst did not respond to the change in cross-linking density as much. The trend can be seen in entries 6–8, as the catalyst prepared with 1 or 0.5 DVB gave essentially the same rate constant within our experimental error. Without DVB, Zn-MINP(**4a**) was actually a slightly worse catalyst than Zn-MINP(**4d**) (entries 3 and 8). Apparently, when the MINP core was too flexible, the imprinting effect became very weak.

The above results suggest that, to successfully transfer the structural information from the template to the active site and then to the catalysis, we need a significant cross-linking density in the MINP core but too rigid an active site lowers the efficiency of the catalyst. It is illuminating to see that 0.5 equiv DVB in the MINP preparation afforded not only the highest activity (entries 1–3) but also the highest selectivity (compare entries 2 and 7) in catalysis. The result suggests that catalytic activity did not have to suffer at the expense of the selectivity in our artificial esterases, at least in the current example.

Substrates **6** and **7** differ from PNPH in the alkyl and phenyl side, respectively. The difference was especially subtle in **6** where a methyl group moved from the chain end by one carbon in comparison to PNPH. Yet, both substrates were completely inactive in the presence of Zn-MINP(**4a**), highlighting the selectivity of our synthetic esterase (entries 9–10).[43] It seems the Zn-MINP was far more sensitive to the structure of substrates during catalysis than to the structure of guests during binding (**4a** and **4d**). The results are reasonable, because binding between a receptor and its ligand is a single event, whereas conversion of a substrate to the product by a catalyst requires many turnovers and may have amplified the difference. In our recent studies, MINP receptors were able to distinguish leucine and isoleucine which also differ by the position of a single methyl,[31] as well as mono- and oligosaccharides that differ by the inversion of a single hydroxyl.[30,32] We were pleased to see that similar precision was observed in catalysis.

The active site of Zn-MINP(**4a**) was designed to bind PNPH precisely. Thus, it should be able to distinguish substrates with a shorter or longer acyl chain. Without any catalysts, the hydrolysis of *p*-nitrophenyl ester slowed down as the acyl chain went from C2 to C8 (Table 2, entries 14–17). The MINP-catalyzed reactions, however, followed the order of C6 > C2 > C8 > C4 with a ratio of 1 : 0.16 : 0.13 : 0.11 (compare entry 2 with entries 11–13). The selectivity of the catalyst seemed to result from both the preference of the catalyst for PNPH and the inherent reactivity.[44] Thus, the catalyst was able to pick the correct substrate from very similar structural analogues. Take PNPA and PNPH as examples. The inherent reactivity of the two esters was PNPA/PNPH = 3/1 but the catalyst reversed the reactivity, to PNPA/PNPH = 1/6.

The chain-length selectivity of our catalyst was highlighted by a competition experiment. The data points in open circles (○) in Figure 2 indicate the hydrolysis of 40 μM butyrate **9** catalyzed by 8 μM Zn-MINP(**4a**). The reaction was quite slow as expected, shown by the small increase of absorbance at 400 nm for the *p*-nitrophenoxide. For the data points in triangles (△), 40 μM **9** was added in the beginning and then again at 30 min. The higher absorbance came from a higher total concentration of the substrate in the solution. For the data points in squares (□), 40 μM **9** was added in the beginning but 40 μM PNPH was added to the solution at 30 min. The absorbance immediately began to rise after the PNPH addition, consistent with the selectivity of the catalysts for the C6 substrate.

Since the branched template **4d** resembled the branched substrate **6**, it is not surprising that Zn-MINP(**4d**) displayed good activity in the hydrolysis of **6** (entries 18–20). The balance of rigidity and flexibility was observed once again, and 0.5 equiv DVB afforded the highest activity. With this catalyst, **6** became more reactive than PNPH

(compare entries 19 and 7, for example). Thus, we can tune the reactivity of the linear and the branched substrates at will, using the MINP catalyst with the matched active site.

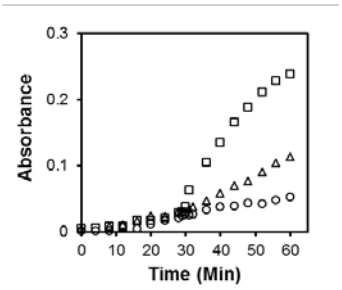

Figure 2. Absorbance at 400 nm as a function of time for the hydrolysis of 40 μM 4-nitrophenyl butyrate (**9**) catalyzed by Zn-MINP(**4a**) in a 25 mM HEPES buffer (pH 7.0) at 40 °C (○). In the data series marked with squares (□), 40 μM PNPH was added again at 30 min. In the data series marked with triangles (△), 40 μM PNPH was added at 30 min. [MINP(**4a**)] = 8 μM.

Michaelis-Menten kinetics of Zn Catalysts. Zn-MINP(**4a**) displayed enzyme-like behavior in its hydrolysis, following Michaelis-Menten kinetics at different pH values (Table 3).[45] The artificial zinc enzyme gave K_m = 0.09 mM and k_{cat} = 3.4 × 10^{-3} S^{-1} at pH 8 (entry 3), comparable to those of a natural zinc enzyme (bovine carbonic anhydrase or BCA) under the same conditions (entry 7). Although there could be enzymes and modified enzymes with higher activities for *p*-nitrophenyl esters,[46,47] BCA was often used as the point of reference for artificial zinc enzymes because of its catalytic zinc in the active site.[8-13] In our hands, due to the slightly stronger binding of the substrate, the catalytic efficiency (k_{cat}/K_m) of Zn-MINP(**4a**) more than doubled that of the natural enzyme (entries 3 and 7).

Table 3. Michaelis-Menten parameters for the hydrolysis of PNPH catalyzed by Zn-MINP(4a) at different pHs.[a]

Entry	pH	V_{max} (× 10^{-7} mol/s)	K_m (mM)	k_{cat} (× 10^{-3} s^{-1})	k_{cat}/K_m ($M^{-1}s^{-1}$)
1	7.0	0.42 ± 0.04	0.21 ± 0.003	5.19 ± 0.44	25
2	7.5	0.33 ± 0.03	0.16 ± 0.01	4.15 ± 0.35	26
3	8.0	0.27 ± 0.05	0.09 ± 0.009	3.40 ± 0.65	38
4	8.5	0.92 ± 0.10	0.07 ± 0.01	11.5 ± 1.5	160
5	9.5	2.19 ± 0.09	0.13 ± 0.01	27.3 ± 1.3	210
6	10	2.98 ± 0.28	0.17 ± 0.01	36.5 ± 3.8	220
7	8.0[b]	0.33 ± 0.03	0.23 ± 0.04	4.15 ± 0.35	18
8	8.0[c]	1.04 ± 0.05	0.14 ± 0.01	13.0 ± 0.7	93

[a] The hydrolysis was catalyzed by [Zn-MINP(**4a**)] in 25 mM HEPES buffer at 40 °C unless indicated otherwise. [Zn-MINP(**4a**)] = 8.0 μM. [b] The hydrolysis was catalyzed by bovine carbonic anhydrase (BCA) in 25 mM HEPEs buffer (pH 8.0) at 40 °C. [BCA] = 8.0 μM. [c] The catalyst was Zn-MINP(**4a**/**11**).

With the background rate constants (k_{uncat}) measured at 0.07 × 10^{-4} S^{-1} at pH 7 and 0.15 × 10^{-4} S^{-1} at pH 8), the rate acceleration factor (k_{cat}/k_{uncat}) was calculated to be 740 at pH 7 and 230 at pH 8. The catalytic proficiency—(k_{cat}/K_m)/k_{uncat}—was 3.5 × 10^6 M^{-1} at pH 7 and 2.6 × 10^6 M^{-1} at pH 8.

We also found that the coordination environment of the zinc also influenced the catalysis. Zn-MINP(**4a**/**11**) was prepared using amine **4a** as the template but a different zinc complex (**11**) as the FM. As shown by the kinetic data (entry 8), this artificial zinc enzyme exhibited a higher activity than either the original Zn-MINP(**4a**) or BCA, with a calculated k_{cat}/k_{uncat} value of 870 at pH 8.

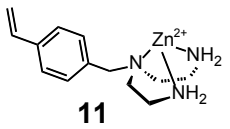

11

The pH profile of the hydrolysis of PNPH by Zn-MINP(**4a**) is shown in Figure 3. The profile is similar to the peptide-based artificial zinc enzymes reported in the literature.[8-13] The curve suggests a single protonation/deprotonation step for the active-site water with a pK_a of 8.36 ± 0.15. The number is higher than those of zinc-bound water in carbonic anhydrase B and C (6.8–7.3)[48] but comparable to those of other artificial zinc enzymes.[8-13]

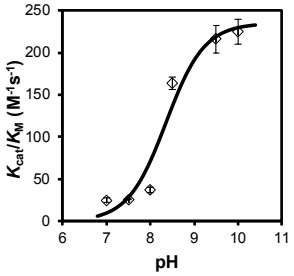

Figure 3. pH dependence of the hydrolysis of PNPH by Zn-MINP(**4a**). The smooth curve was obtained by nonlinear least-squares curve fitting to the equation, $k_{cat}/K_m = (k_{cat}/K_m)_{max} \times 10^{-pKa}/(10^{-pH} + 10^{-pKa})$, with the inflection point corresponding to the pK_a of the zinc-bound water (8.36 ± 0.15).[12]

One of the challenges with previous artificial zinc enzymes was product inhibition,[8] because the products (carboxylates and phenoxides) are stronger ligands for zinc than the starting materials (water and ester). Figure 4a shows the catalytic activity of 0.2 μM Zn-MINP(**4a**) in the presence of a large excess of PNPH (100 μM). Figure 4b shows the amount of product formed as a function of time. The amount was calculated based on an extinction coefficient of ε_{400} = 0.0216 μM^{-1} cm^{-1} for *p*-nitrophenoxide at pH 8.0. A turnover number of 324 was calculated at 300 min. At pH 7, the turnover number was found to be 460 at 540 min.[49] Even at high conversion (>95%), the reaction showed very little signs of slowing down (Figure S37). Our design gives an active site precisely constructed for the substrate (PNPH). Although carboxylate and the phenoxide should coordinate better to a cationic zinc more strongly than the starting materials, the active site of MINP(**4a**) must have prevented their complexation, possibly because the preferred coordination geometry could not be achieved in the tight binding site.

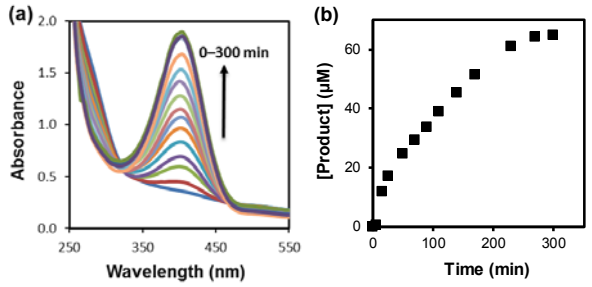

Figure 4. (a) UV-Vis spectra of PNPH (100 μM) in a 25 mM HEPEs buffer (pH 8.0) at 40 °C, after addition of 0.2 μM Zn-MINP(**4a**). (b) Amount of *p*-nitrophenoxide formed as a function of time, calculated based on an extinction coefficient of $\varepsilon_{400} = 0.0216\ \mu M^{-1}\ cm^{-1}$.

Table 4 compares the catalytic performance of the Zn-MINP catalysts with artificial zinc enzymes reported in the literature, at comparable pHs if the corresponding data were available. Since small-molecule zinc enzyme mimics typically have poor catalytic turnovers, we only included peptidic catalysts that have displayed the Michaelis-Menten kinetics and good catalytic activities.[8-13] Although our Zn-MINPs were designed specifically for PNPH and the other artificial zinc enzymes were only tested for PNPA, the comparison gives a reasonable perspective on our catalysts, given that PNPH is generally less reactive than PNPA in the absence of catalysts (vide supra).

Table 4. Catalytic data for the hydrolysis of PNPA catalyzed by artificial zinc enzymes.[a]

Entry	Catalysts	pH	pK_a	k_{cat}/K_m ($M^{-1}s^{-1}$)	TON
1[9]	MID1-Zn	8	8.2	180	>50
2[8]	Modified TRI peptide-Zn[b]	8	8.8	3	>10
3[12]	Ac-IHIHIQI-$CONH_2$	8	9.3	62	>20
4[11]	^{A104}AB3	9	9.0	32	-
5[13]	CC-Hept–Cys–His–Glu	8	9.0	18	>12
6	Zn-MINP(**4a**) for PNPH	8	8.4	38	>320 (>460)[c]
7	Zn-MINP(**4a**/**11**) for PNPH	8	-	93	-

[a] The data for the artificial zinc enzymes reported in the literature were obtained at 22–25 °C for PNPA and the data for the Zn-MINPs at 40 °C for PNPH. [b] The catalyst was $[Hg(II)]_S[Zn(II)(H_2O/OH^-)]_N(TRIL9CL23H)_3^{n+}$. [c] The turnover number in parentheses was obtained at pH 7 at 540 min.

Generally speaking, the pK_a of the zinc-bound water was on the low side for our Zn-MINPs among their peers and the catalytic efficiency on the medium to high side, depending on the nature of the tridentate ligand used in the Zn-MINPs (Table 4). Although the TON numbers reported were the minima in all cases, our catalysts certainly looked very favorable in this property that has been a particular challenge with traditional artificial zinc enzymes. [8]

CONCLUSIONS

In summary, through micellar imprinting, we could prepare zinc-based artificial enzymes from simple building blocks in a highly efficient manner. The entire synthesis and purification could be done in less than 2 days once all the starting materials are available. The catalyst displayed enzyme-like kinetics and pH profile, and was able to distinguish the position of a single methyl group and the chain length of the substrate, as well as substitution pattern of the phenyl group. High turnovers were achieved as the active site prevented the products from re-binding the zinc.

The most significant feature of our artificial enzymes is the ability to fine-tune the size and shape of the active site in a rational manner, as well as the position of the catalytic metal ion with respect to the reactive functionality. These features gave us an unusual level of control in the construction of active site and allowed us to switch the relative reactivity of substrates with similar intrinsic reactivities. Although one wishes to move beyond activated esters in the catalytic hydrolysis,[50] efficient construction of a substrate-specific functionalized active site is important to the development of any artificial enzymes. The principle demonstrated in this study should not be limited to hydrolysis and could be used to design other biomimetic catalysts with enzyme-like activity and selectivity.

ASSOCIATED CONTENT

Supporting Information

Experimental details, ITC titration curves, Michaelis-Menten data, and additional figures. This material is available free of charge via the Internet at http://pubs.acs.org.

AUTHOR INFORMATION

Corresponding Author

zhaoy@iastate.edu

Notes

The authors declare no competing financial interests.

ACKNOWLEDGMENT

We thank NSF (DMR-1464927 and CHE-1708526) for financial support of this research.

REFERENCES

(1) Auld, D. S.: In *Encylopedia of Inorganic Chemistry, 2nd Ed.*; King, R. B., Ed.; Wiley: New York, 2007; pp 5885-5927.
(2) Vallee, B. L.; Auld, D. S. Zinc: Biological Functions and Coordination Motifs. *Acc. Chem. Res.* **1993**, *26*, 543-551.
(3) Vallee, B. L.; Auld, D. S. Zinc Coordination, Function, and Structure of Zinc Enzymes and Other Proteins. *Biochemistry* **1990**, *29*, 5647-5659.
(4) Coleman, J. E. Zinc Enzymes. *Curr. Opin. Chem. Biol.* **1998**, *2*, 222-234.
(5) Parkin, G. Synthetic Analogues Relevant to the Structure and Function of Zinc Enzymes. *Chem. Rev.* **2004**, *104*, 699-768.
(6) Kimura, E.; Hashimoto, H.; Koike, T. Hydrolysis of Lipophilic Esters Catalyzed by a Zinc(II) Complex of a Long Alkyl-Pendant Macrocyclic Tetraamine in Micellar Solution. *J. Am. Chem. Soc.* **1996**, *118*, 10963-10970.
(7) Vahrenkamp, H. Transitions, Transition States, Transition State Analogues: Zinc Pyrazolylborate Chemistry Related to Zinc Enzymes. *Acc. Chem. Res.* **1999**, *32*, 589-596.
(8) Zastrow, M. L.; Peacock, A. F. A.; Stuckey, J. A.; Pecoraro, V. L. Hydrolytic Catalysis and Structural Stabilization in a Designed Metalloprotein. *Nat. Chem.* **2012**, *4*, 118-123.
(9) Der, B. S.; Edwards, D. R.; Kuhlman, B. Catalysis by a De Novo Zinc-Mediated Protein Interface: Implications for Natural Enzyme Evolution and Rational Enzyme Engineering. *Biochemistry* **2012**, *51*, 3933-3940.
(10) Zastrow, M. L.; Pecoraro, V. L. Influence of Active Site Location on Catalytic Activity in De Novo-Designed Zinc Metalloenzymes. *J. Am. Chem. Soc.* **2013**, *135*, 5895-5903.

(11) Song, W. J.; Tezcan, F. A. A Designed Supramolecular Protein Assembly with in Vivo Enzymatic Activity. *Science* **2014**, *346*, 1525-1528.
(12) Rufo, C. M.; Moroz, Y. S.; Moroz, O. V.; Stohr, J.; Smith, T. A.; Hu, X. Z.; DeGrado, W. F.; Korendovych, I. V. Short Peptides Self-Assemble to Produce Catalytic Amyloids. *Nat. Chem.* **2014**, *6*, 303-309.
(13) Burton, A. J.; Thomson, A. R.; Dawson, W. M.; Brady, R. L.; Woolfson, D. N. Installing Hydrolytic Activity into a Completely De Novo Protein Framework. *Nat. Chem.* **2016**, *8*, 837-844.
(14) Awino, J. K.; Zhao, Y. Protein-Mimetic, Molecularly Imprinted Nanoparticles for Selective Binding of Bile Salt Derivatives in Water. *J. Am. Chem. Soc.* **2013**, *135*, 12552-12555.
(15) Wulff, G. Enzyme-Like Catalysis by Molecularly Imprinted Polymers. *Chem. Rev.* **2001**, *102*, 1-28.
(16) Wulff, G.; Liu, J. Design of Biomimetic Catalysts by Molecular Imprinting in Synthetic Polymers: The Role of Transition State Stabilization. *Acc. Chem. Res.* **2012**, *45*, 239-247.
(17) Emgenbroich, M.; Wulff, G. A New Enzyme Model for Enantioselective Esterases Based on Molecularly Imprinted Polymers. *Chem.-Eur. J.* **2003**, *9*, 4106-4117.
(18) Maddock, S. C.; Pasetto, P.; Resmini, M. Novel Imprinted Soluble Microgels with Hydrolytic Catalytic Activity. *Chem. Commun.* **2004**, 536-537.
(19) Liu, J.-q.; Wulff, G. Functional Mimicry of Carboxypeptidase a by a Combination of Transition State Stabilization and a Defined Orientation of Catalytic Moieties in Molecularly Imprinted Polymers. *J. Am. Chem. Soc.* **2008**, *130*, 8044-8054.
(20) Carboni, D.; Flavin, K.; Servant, A.; Gouverneur, V.; Resmini, M. The First Example of Molecularly Imprinted Nanogels with Aldolase Type I Activity. *Chem. -Eur. J.* **2008**, *14*, 7059-7065.
(21) Kirsch, N.; Hedin-Dahlström, J.; Henschel, H.; Whitcombe, M. J.; Wikman, S.; Nicholls, I. A. Molecularly Imprinted Polymer Catalysis of a Diels-Alder Reaction. *J. Mol. Catal. B: Enzym.* **2009**, *58*, 110-117.
(22) Chen, Z. Y.; Xu, L.; Liang, Y.; Zhao, M. P. Ph-Sensitive Water-Soluble Nanospheric Imprinted Hydrogels Prepared as Horseradish Peroxidase Mimetic Enzymes. *Adv. Mater.* **2010**, *22*, 1488-1492.
(23) Servant, A.; Haupt, K.; Resmini, M. Tuning Molecular Recognition in Water-Soluble Nanogels with Enzyme-Like Activity for the Kemp Elimination. *Chem.-Eur. J.* **2011**, *17*, 11052-11059.
(24) Shen, X.; Huang, C.; Shinde, S.; Jagadeesan, K. K.; Ekström, S.; Fritz, E.; Sellergren, B. Catalytic Formation of Disulfide Bonds in Peptides by Molecularly Imprinted Microgels at Oil/Water Interfaces. *ACS Appl. Mater. Interfaces* **2016**, *8*, 30484-30491.
(25) Zimmerman, S. C.; Lemcoff, N. G. Synthetic Hosts Via Molecular Imprinting—Are Universal Synthetic Antibodies Realistically Possible? *Chem. Commun.* **2004**, 5-14.
(26) Zhang, S.; Zhao, Y. Facile Synthesis of Multivalent Water-Soluble Organic Nanoparticles Via "Surface Clicking" of Alkynylated Surfactant Micelles. *Macromolecules* **2010**, *43*, 4020-4022.
(27) Awino, J. K.; Zhao, Y. Imprinted Micelles for Chiral Recognition in Water: Shape, Depth, and Number of Recognition Sites. *Org. Biomol. Chem.* **2017**, *15*, 4851-4858.
(28) Gunasekara, R. W.; Zhao, Y. Intrinsic Hydrophobicity Versus Intraguest Interactions in Hydrophobically Driven Molecular Recognition in Water. *Org. Lett.* **2017**, *19*, 4159-4162.
(29) Fa, S.; Zhao, Y. Peptide-Binding Nanoparticle Materials with Tailored Recognition Sites for Basic Peptides. *Chem. Mater.* **2017**, *29*, 9284-9291.
(30) Awino, J. K.; Gunasekara, R. W.; Zhao, Y. Selective Recognition of D-Aldohexoses in Water by Boronic Acid-Functionalized, Molecularly Imprinted Cross-Linked Micelles. *J. Am. Chem. Soc.* **2016**, *138*, 9759-9762.
(31) Awino, J. K.; Gunasekara, R. W.; Zhao, Y. Sequence-Selective Binding of Oligopeptides in Water through Hydrophobic Coding. *J. Am. Chem. Soc.* **2017**, *139*, 2188-2191.
(32) Gunasekara, R. W.; Zhao, Y. A General Method for Selective Recognition of Monosaccharides and Oligosaccharides in Water. *J. Am. Chem. Soc.* **2017**, *139*, 829-835.
(33) Duan, L.; Zhao, Y. Selective Binding of Folic Acid and Derivatives by Imprinted Nanoparticle Receptors in Water. *Bioconjugate Chem.* **2018**, *29*, 1438-1445.
(34) Awino, J. K.; Zhao, Y. Molecularly Imprinted Nanoparticles as Tailor-Made Sensors for Small Fluorescent Molecules. *Chem. Commun.* **2014**, *50*, 5752-5755.
(35) Fa, S.; Zhao, Y. Water-Soluble Nanoparticle Receptors Supramolecularly Coded for Acidic Peptides. *Chem. -Eur. J.* **2018**, *24*, 150-158.
(36) Matsui, J.; Higashi, M.; Takeuchi, T. Molecularly Imprinted Polymer as 9-Ethyladenine Receptor Having a Porphyrin-Based Recognition Center. *J. Am. Chem. Soc.* **2000**, *122*, 5218-5219.
(37) Becker, J. J.; Gagné, M. R. Exploiting the Synergy between Coordination Chemistry and Molecular Imprinting in the Quest for New Catalysts. *Acc. Chem. Res.* **2004**, *37*, 798-804.
(38) Muratsugu, S.; Tada, M. Molecularly Imprinted Ru Complex Catalysts Integrated on Oxide Surfaces. *Acc. Chem. Res.* **2013**, *46*, 300-311.
(39) Schmidtchen, F. P.: Isothermal Titration Calorimetry in Supramolecular Chemistry. In *Supramolecular Chemistry: From Molecules to Nanomaterials*; Steed, J. W., Gale, P. A., Eds.; Wiley: Online, 2012.
(40) Awino, J. K.; Zhao, Y. Polymeric Nanoparticle Receptors as Synthetic Antibodies for Nonsteroidal Anti-Inflammatory Drugs (NSAIDs). *ACS Biomater. Sci. Eng.* **2015**, *1*, 425-430.
(41) In our synthesis, we assumed the tridentate ligand in **5** was able to retain the zinc during the preparation and purification of the MINPs. Consistent with the notion, hydrolysis of PNPH by Zn-MINP(**4a**) showed no improvement upon the addition of up to 20 equiv of Zn^{2+} (Figure S20, Table S2), suggesting that the active site was fully metallated in Zn-MINP(**4a**).
(42) The Zn-MINP complex showed no catalytic activity for unactivated para-isopropylphenyl hexanoate under similar experimental conditions.
(43) In our hands, when the activated ester was not hydrolyzed, the absorbance at 400 nm often displayed small, negative changes over time (Figures S21-S22, presumably caused by the scattering of UV light by the phase-separated ester starting material, due to its hydrophobicity.
(44) The difference between the C4 and C8 *p*-nitrophenyl esters was within experimental error.
(45) The numbers were obtained from linear curve-fitting to the Lineweaver-Burk plots (Figures S23-29). The data were mostly within 20% of those obtained by directing fitting to the Michaelis-Menten equation (Table S3, Figures S30-36).
(46) Yano, Y.; Shimada, K.; Okai, J.; Goto, K.; Matsumoto, Y.; Ueoka, R. Fairly Marked Enantioselectivity for the Hydrolysis of Amino Acid Esters by Chemically Modified Enzymes. *J. Org. Chem.* **2003**, *68*, 1314-1318.
(47) Engström, K.; Nyhlén, J.; Sandström, A. G.; Bäckvall, J.-E. Directed Evolution of an Enantioselective Lipase with Broad Substrate Scope for Hydrolysis of A-Substituted Esters. *J. Am. Chem. Soc.* **2010**, *132*, 7038-7042.
(48) Verpoorte, J. A.; Mehta, S.; Edsall, J. T. Esterase Activities of Human Carbonic Anhydrases B and C. *J. Biol. Chem.* **1967**, *242*, 4221-4229.
(49) We did not attempt to achieve even higher turnover numbers due to the limited solubility of PNPH in aqueous buffer.
(50) Menger, F. M.; Ladika, M. Origin of Rate Accelerations in an Enzyme Model: The P-Nitrophenyl Ester Syndrome. *J. Am. Chem. Soc.* **1987**, *109*, 3145-3146.